Synthesis of peptidoglycan and membrane during the division cycle of rod-shaped, gram-negative bacteria

Synthesis of peptidoglycan and membrane during the division cycle of rod-shaped, gram-negative bacteria.

D Gally, K Bray and S Cooper
J. Bacteriol. **1993, 175(10):3121.**

JOURNAL OF BACTERIOLOGY, May 1993, p. 3121–3130
0021-9193/93/103121-10$02.00/0

Vol. 175, No. 10

Synthesis of Peptidoglycan and Membrane during the Division Cycle of Rod-Shaped, Gram-Negative Bacteria

DAVID GALLY,† KELVIN BRAY, AND STEPHEN COOPER*

Department of Microbiology and Immunology, University of Michigan Medical School, Ann Arbor, Michigan 48109-0620

Received 4 December 1992/Accepted 14 March 1993

A modified procedure for determining the pattern of peptidoglycan synthesis during the division cycle has allowed the measurement of the rate of side wall synthesis during the division cycle without the contribution due to pole formation. As predicted by a model proposing that the surface growth of the cell is regulated by mass increase, we find a decrease in side wall synthesis in the latter half of the division cycle. This supports the proposal that, upon invagination, pole growth accommodates a significant proportion of the increasing cell mass and that residual side wall growth occurs in response to the residual mass increase not accommodated by pole volume. The observed side wall synthesis patterns support the proposal that mass increase is a major, and possibly sole, regulator of bacterial surface increase. Membrane synthesis during the division cycle of the gram-negative, rod-shaped bacteria *Escherichia coli* and *Salmonella typhimurium* has also been measured with similar methods. The rate of membrane synthesis—measured by incorporation of radioactive glycerol or palmitate relative to simultaneous labeling with radioactive leucine—exhibits the same pattern as peptidoglycan synthesis. The results are compatible with a model of cell surface growth containing the following elements. (i) During the period of the division cycle prior to invagination, growth of the cell occurs predominantly in the side wall and the cell grows only in length. (ii) When invagination begins, pole growth accommodates some cytoplasmic increase, leading to a concomitant decrease in side wall synthesis. (iii) Surface synthesis increases relative to mass synthesis during the last part of the division cycle because of pole formation. It is proposed here that membrane synthesis passively follows the pattern of peptidoglycan synthesis during the division cycle.

How is the rate of cell surface synthesis regulated in bacteria? One proposal consistent with the available data is that the surface of the gram-negative, rod-shaped cell grows in response to the increase in cell mass. This proposal has been termed the surface stress model (12; see reference 13 for discussion and recent references). The continuous increase in the cytoplasmic constituents of a cell (RNA, protein, water, and ions, etc.) leads to an increase in turgor pressure on the cell surface. This increase in turgor pressure leads to the stressing and bending of peptidoglycan bonds. The cell surface expands when nascent material is incorporated into the stress-bearing plane upon the preferential scission of the stressed peptidoglycan linkages. Thereby, new wall growth responds to and accommodates the increase in mass or volume. The slight reduction in turgor resulting from the incorporation of new material into the stressed layer allows cell mass to again increase prior to further surface growth. The continuous and exponential increase in cell mass or cytoplasm leads to the continuous increase in cell surface.

It has been proposed that the murein of gram-negative, rod-shaped bacteria enlarges solely in response to the increase in cell cytoplasm. Evidence for this proposal was obtained by using the backwards-ratio-of-rates method with the membrane elution technique (2, 4, 5, 7). The rate of synthesis of peptidoglycan during the division cycle was measured by comparing the rate of incorporation of leucine to the rate of incorporation of a peptidoglycan precursor such as diaminopimelic acid (DAP) or *N*-acetylglucosamine. The ratio was constant for bacteria prior to invagination and increased in the latter part of the division cycle (2, 7). This model of wall growth would explain the constant cell density observed during the division cycle (14). This is because the derivations of the parameters of wall growth were specifically chosen to give an exponential increase in cell volume and not to produce any particular pattern for the increase in cell surface.

One prediction of the mass-determined model of wall growth (2) is that side wall synthesis will decrease during invagination. This predicted drop was not observed in previous experiments with the membrane elution method (2, 7). Electron microscopic autoradiographic analysis of wall synthesis has shown that cells undergoing constriction exhibit decreased amounts of side wall label compared with nonconstricting cells (17). In this electron microscope experiment, the autoradiographic measurements were made on a population of cells on a grid, and thus experimental variables were minimized. However, the precise rate of side wall synthesis as a function of cell age could not be determined.

A drop in the ratio of side wall label to protein label during a pulse incorporation would be expected to be observed at later generations of elution from the membrane elution apparatus when the obscuring effects of labeled poles are removed from consideration. The evidence indicates that bacteria remain permanently bound at their site of attachment to the membrane (4), so that the newly synthesized poles in the middle of the cell are lost in the first two generations of elution. Although we feel that this assumption is well supported by the evidence, we would observe that it is not yet unequivocally proven that all pole material is lost during the first two generations and that no labeled pole is found bound to the membrane. After this loss of labeled pole (i.e., the third generation of elution and beyond), it should be

* Corresponding author. Electronic mail address: STEPHEN-COOPER@UM.CC.UMICH.EDU.

† Present address: Department of Microbiology and Immunology, Bowman Gray Medical School, Winston-Salem, NC 27157-1064.

possible to measure the rate of side wall synthesis. To be precise, the side wall synthesis being measured is the wall being synthesized in the culture during the period of labeling and prior to being placed on the membrane. The membrane elution method merely enables one to determine the pattern of synthesis during the division cycle by analyzing cells eluted from the membrane. Throughout this analysis, we will assume that the variations we observe after the first two generations of elution are due to variations in the pattern of incorporation of label into the side wall of the cell.

In addition to peptidoglycan, the cell surface of gram-negative, rod-shaped cells has a membranous component on both sides of the peptidoglycan. The analysis of the pattern of membrane synthesis during the division cycle has generally proceeded without explicitly considering the pattern of peptidoglycan synthesis. There have been numerous studies carried out to determine the pattern of membrane synthesis during the division cycle (reviewed in reference 5). Earlier experiments with the membrane elution technique gave results that were interpreted as a bilinear pattern of phospholipid synthesis (15). More recently, a doubling in the rate of phospholipid synthesis during the division cycle was proposed on the basis of experiments with bacteria synchronized by using repeated phosphate starvations (9, 10). This doubling has been proposed to represent a doubling in membrane synthetic sites, possibly related to the appearance of periseptal annuli, but no temporal connection has been found (11).

Here, we demonstrate that the pattern of side wall synthesis during the third and subsequent cycles of elution from the membrane elution apparatus is consistent with the predictions of the surface stress model. Specifically, it is shown that during the latter part of the division cycle, there is a decrease in the rate of side wall synthesis. The labeling pattern observed fits the predictions of a model in which pole increase accommodates mass increase and leads to a concomitant decrease in side wall synthesis (2, 4). In addition, we compare membrane synthesis with peptidoglycan synthesis during the division cycle. The attachment of inner and outer membranes to the load-bearing peptidoglycan layer implies that the membrane might exhibit the same pattern of expansion and synthesis as peptidoglycan during the division cycle. The experiments described here support this proposal. The observed pattern of surface synthesis is consistent with the predictions of cell expansion driven by mass increase.

MATERIALS AND METHODS

Bacteria and growth conditions. *Salmonella typhimurium* 2616 (*lysA* mutant) (from K. E. Sanderson, the University of Calgary) and *Escherichia coli* NC3 were grown in C medium ([per liter] 3 g of NaCl, 3 g of KH_2PO_4, 2 g of NH_4Cl, 6 g of Na_2HPO_4, 0.25 g of $MgSO_4$) supplemented with 50 μg of lysine per ml and either 0.4% glucose or 0.4% glycerol. All bacteria were grown at 37°C with rotary shaking.

Radioactive compounds. Tritium-labeled DAP (*meso*-2,6-diamino-[3,4,5-^{3}H]pimelic acid; 23 Ci/mmol) was obtained from Research Products International Corp., Mt. Prospect, Ill. Tritium-labeled *N*-acetylglucosamine (*N*-[1,6-^{3}H]acetylglucosamine; 30 Ci/mmol), glycerol ([2-^{3}H]glycerol; 20 Ci/mmol), palmitate ([9,10-^{3}H(N)]palmitate; 60 Ci/mmol), and carbon-labeled leucine ([1-^{14}C]leucine; 55 Ci/mmol) were obtained from American Radiolabeled Chemicals Inc., St. Louis, Mo.

Pulse-radiolabeling of bacteria for membrane elution experiments. For all membrane elution work, the bacteria were grown exponentially for over 10 generations before labeling. In all experiments, a double-label design was utilized so that the incorporation of the tritium compound of interest was compared with the incorporation of a ^{14}C-labeled amino acid; it is leucine in these experiments, but all amino acids tested give the same exponential pattern (3). Bacteria (100 ml) were labeled at a concentration of approximately 1.0×10^8 cells per ml. The two labels (^{3}H-labeled cell surface component precursor and [^{14}C]leucine) were mixed in C medium prior to addition to the culture. [^{3}H]DAP was primarily used for determination of the pattern of peptidoglycan synthesis during the division cycle, with confirmatory experiments performed with *N*-[^{3}H]acetylglucosamine. Lysine (50 μg/ml) was present during the growth of *Escherichia coli* NC3 in order to reduce the conversion of DAP to lysine. For the determinations of the rate of membrane synthesis in *E. coli* NC3, [2-^{3}H]glycerol or [9,10-^{3}H(N)]palmitate was used. Glycerol labeled on the 2 position is most stable and thus is the best for labeling lipids (7a). For *S. typhimurium* 2616, only [^{3}H]palmitate was used because this strain produced a more defined elution profile when grown with glycerol as the principal carbon and energy source. Total lipid extraction measurements were performed by the method of Bligh and Dyer (1).

Division cycle analysis with the membrane elution method (backwards analysis). The theory behind this method has been thoroughly described previously (4). Bacteria were pulse-labeled and filtered onto a membrane, which was then inverted, and newborn cells were eluted from the membrane with fresh medium. Bacteria were analyzed as a function of time of elution. Three modifications in the procedure appear to allow the measurements reported below. First, after the bacteria had been placed on the membrane by vacuum filtration, the cells were washed three times with unlabeled medium. The medium was then vigorously swirled to remove unattached bacteria. That is, after swirling, the wash medium was poured off in order to remove the loosely attached cells before inverting the membrane. This washing procedure removed weakly bound bacteria, thus improving the subsequent generations of elution. A similar result has also been noticed by Zaritsky and Helmstetter (18). The second modification was to enclose the entire apparatus in a constant temperature chamber (37°C) and have the fractions automatically removed from the chamber by a pumping system. Eluted bacteria were caught in a funnel and pumped to a fraction collector. This procedure ensures that the membrane elution experiment is undisturbed, with no drafts or other airflow changes affecting growth on the membrane. A third modification was to carry out some experiments at room temperature (22°C). This permitted more time points to be taken during each generation of elution, allowing the timing of cell cycle events to be determined more precisely. Because the label has been removed by filtration onto the membrane, the label incorporated into the cells is measured by mixing the eluate with a water-miscible scintillation fluid and counting the radioactivity. Control experiments have shown that there is no difference between this method and filtering the cells and counting the cells immobilized on filters. By the time the cells are eluted from the membrane, all pool material has been incorporated into cell material, and there is no need to filter the cells. In addition, we have facilitated experiments by using changes in the eluted [^{14}C]leucine counts to define the end of a generation of elution. Previously, generations of elution were determined by monitoring the change in cell number. For experiments in

which elution is monitored for several generations, cell counts may be required every 2 min over a 6-h period. An explanation of how the radioactivity per milliliter can be used to determine generations of elution is presented in Fig. 1a. Because it was possible to determine generations of elution by the [^{14}C]leucine counts per milliliter, some experiments could be completely automated. Once elution began, samples were collected directly into scintillation vials by using a fraction collector and no further monitoring of cell number was required. Control experiments indicate that this method gave results similar to those obtained when cell counts were monitored over the entire experiment. A more objective analysis of the changes in radioactivity per milliliter can be made by plotting the differential of the initial data, as indicated in Fig. 1b. Rather than estimating the midpoint in each decrease (Fig. 1a), one can use the differential plot to see the inflection point in the original data. The differential reaches a minimum at each inflection point. Consequently, generations of elution are calculated from one minimum to the next, from left to right (Fig. 1b). We have also used the differential plot (similar to that described in Fig. 1) of the dual-label ratio to objectively locate discrete changes in the rate of synthesis of different cell surface components within the division cycle.

Details of counting radioactivity, statistical analysis, and differential analysis. The eluted samples were counted in a Beckman model 3801 scintillation counter. This instrument has been calibrated to correct for any differential quench in the samples. The machine monitors the quench, corrects for quench, calculates the spillover of each isotope into the other windows, and then calculates a corrected disintegrations per minute as a final result. Thus, if there was differential quench in the eluted samples (brought about, perhaps, by the different cell numbers in each sample), then the machine would account for this. In any case, analysis of the H number (the numerical indicator of quenching) indicates that the eluted samples are all quenched to the same degree, and therefore any quenching problem is negligible.

All radioactivity was counted to 2% accuracy in both the ^{3}H and ^{14}C channels. Inspection of the elution results indicates that this is sufficient for analysis. Sequential samples show no variation due to low statistical accuracy.

The differential rates were calculated by taking the differences between every other sample value and plotting the differential after normalizing the results by multiplying by a fixed factor. No data were rejected or discarded in this analysis.

RESULTS

Side wall peptidoglycan synthesis during the division cycle. The results of an experiment giving the rate of incorporation of DAP relative to leucine during the division cycle of *E. coli* NC3 are shown in Fig. 2. The culture was labeled with both [^{3}H]DAP and [^{14}C]leucine for 5 min, and the incorporation pattern was determined with the membrane elution method. Samples were collected over 3-min intervals for five generations. The series of peaks in the cell elution profile indicate that the cell age order of elution was maintained for at least five generations (for an analysis of the age distribution of bacteria in a culture and the reflection of this age distribution in the cell elution pattern, see reference 4). There is an exponential decrease in [^{14}C]leucine per cell during elution, confirming previous results showing that the uptake and incorporation of amino acids is exponential during the division cycle (3). The time for [^{14}C]leucine per cell to decrease

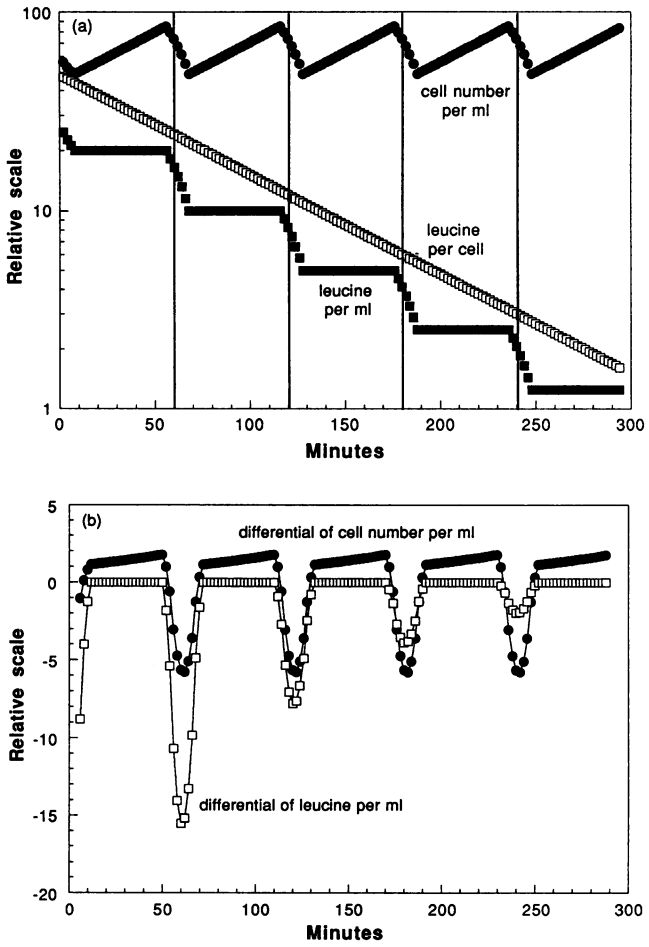

FIG. 1. Determination of generations of elution and timing of changes during the division cycle. (a) Idealized graph of cell number per milliliter, leucine per milliliter, and leucine per cell. The cell elution graph is a sawtooth figure because there are approximately twice as many newborn cells as dividing cells in a culture. The variation in interdivision times leads to the smoothing of the data. For exponential incorporation during the division cycle, as is found with leucine, the leucine per cell graph is as depicted. The leucine per milliliter is a stepwise graph. Dividing the leucine per milliliter by the cell number per milliliter gives the leucine per cell. Notice that one can determine the generation of elution either by the decrease in cell number or by the stepwise decrease in the leucine per milliliter. (b) The running average differential plot of data from panel a. The difference between successive points in the cell number and the leucine per milliliter are plotted. The minima of the two plots occur at the same time and coincide with the decreases shown in the two relevant plots in panel a. Therefore, the generations of elution can be measured from minimum to minimum in the differential plots. (The number of points covering the stepwise decreases in panel b is greater than the number of points apparent in panel a because a running average of three points is taken to smooth out small variations in the experimental data.) When an automated membrane elution experiment is run, cell numbers are not taken after one generation, and the successive generations of elution are indicated solely by the changes in the leucine per milliliter value. It can be seen that the idealized cell number per milliliter profile from panel a gives a repetitive pattern of sharp troughs, all of the same size. Although the running differential of the amino acid elution profile gives the troughs at the same times, the size of the troughs is reduced by a factor of 2 for each generation of elution. This is because the steps in panel a decrease in value by a factor of 2 for each consecutive generation of elution.

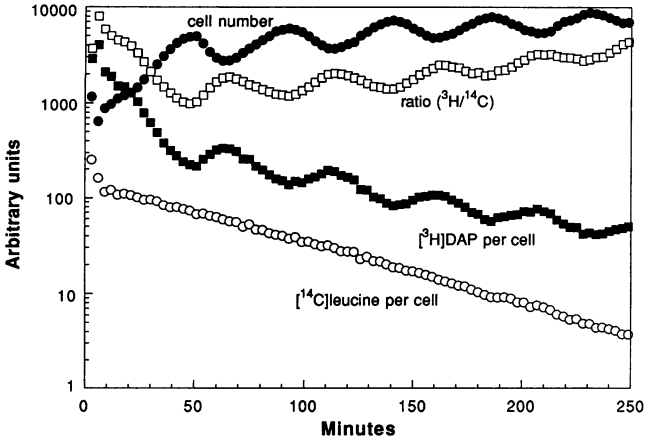

FIG. 2. Pattern of elution of DAP and leucine in *E. coli* NC3. A culture (100 ml) with a cell concentration of 1×10^8 bacteria per ml was labeled for 5 min with [^{3}H]DAP (0.05 nmol/ml; 1.1 μCi/ml) and [^{14}C]leucine (0.5 nmol/ml; 0.03 μCi/ml). The membrane elution experiment was set up as described in Materials and Methods. Each cycle of elution is taken to start at the midpoint in the decrease in cell number. The graph shows five generations of elution. The leucine per cell is a straight line decrease on the exponential scale, but the DAP counts per cell show cell cycle variation. Consequently, the ^{3}H/^{14}C ratio shows cell cycle variation. This experiment is one of four such similar experiments carried out with *E. coli* NC3.

by half is 50 min, indicating that the doubling time on the membrane is 50 min; this is similar to the growth rate of the cells prior to placement on the membrane elution apparatus. These observations indicate that the bacteria on the membrane are in an unperturbed state, dividing regularly and in age order.

The [^{3}H]DAP per cell elution pattern is different from that of leucine. Although this can be seen from the plot of tritium per cell (Fig. 2), it is also apparent in a plot of the ratio of [^{3}H]DAP to [^{14}C]leucine. There is a cyclic variation in DAP incorporation during the division cycle. The very fact that there is a variation in such a plot indicates that the uptake and, as the labeled pool is small, the incorporation of DAP are different from a purely exponential pattern. This pattern of DAP incorporation relative to leucine was also observed in *S. typhimurium* 2616 (Fig. 3a) and with *N*-[^{3}H]acetylglucosamine incorporation in *E. coli* NC3 (Fig. 3b). (The long-term increase in the ratio of DAP to leucine as seen in Fig. 2 and 4 is the subject of further analysis. Although it cannot be analyzed in detail here, it appears to indicate that synthesis of new peptidoglycan along the side wall is not uniform, but rather is nonuniform, with a peak of synthesis in the middle of the cell. This nonuniform incorporation is considered only in the side wall and should not be related to or confused with the increased central synthesis observed in previous experiments [2, 7, 17]. Previous work has usually proposed uniform incorporation along the side wall with additional central synthesis due to pole formation.)

The generations of elution are marked by the cell elution plot. Each cycle starts at the midpoint in the decrease in cell number. The cells eluted just prior to the midpoint in the decrease in the cell number (reading from left to right) are the progeny of cells labeled as newborn or young cells. The label from the older cells appears in the progeny eluting further to the left (i.e., earlier in the elution pattern) within each generation of elution. This is because the first newborn cells eluted from the membrane are from the oldest cells in the labeled population, and with time, cells that were progressively younger and younger at the time of labeling grow through the division cycle to produce newborn cells (4). As the cell cycle is thus interpreted right to left (youngest to oldest), it can be seen in Fig. 2 that the peak in the ratio of incorporation of peptidoglycan precursor to that of leucine, during the first two generations of elution, occurs towards the end of the cell cycle. It was previously proposed that the peaks in the ratio appearing during the first two generations of elution are due to pole synthesis at the time of labeling (2, 7). This effect will be lost after the second generation of elution. However, it is clear that there are cyclic variations extending into the third, fourth, and fifth generations of elution (Fig. 2 and 3).

It should be noted that the expected elevated peak in the second generation of elution, expected to be due to the elution of the remaining labeled pole material at the start of the second generation, is not as high as expected (2, 7). Its

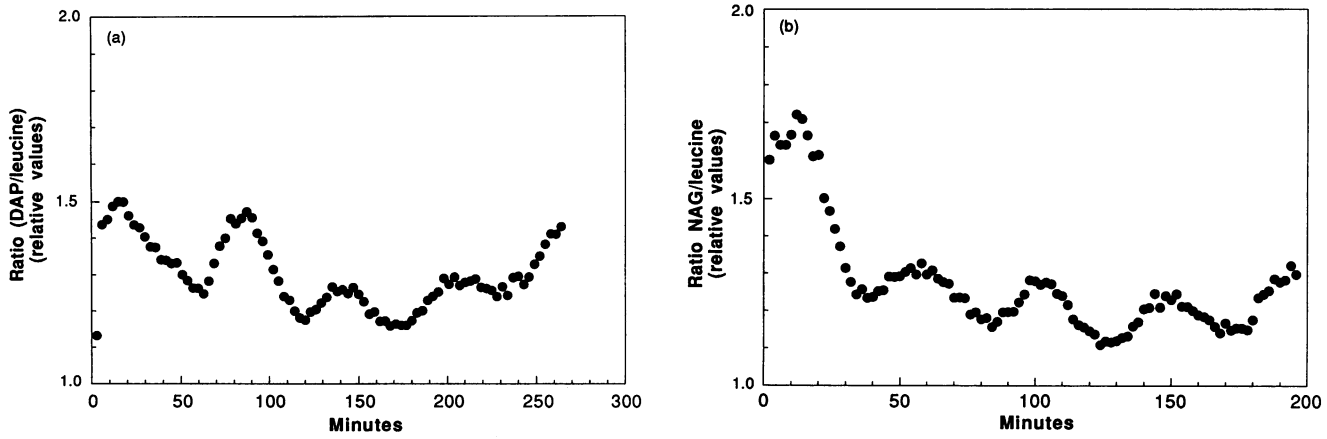

FIG. 3. Peptidoglycan synthesis in *S. typhimurium*. (a) Elution ratio of [^{3}H]DAP to [^{14}C]leucine in *S. typhimurium* 2616. Cell cycle variation in the ratio is shown extending for at least four generations (●). The leucine per cell elution profile for this experiment was a straight line decrease when plotted with an exponential scale, indicating that the cyclic variation is due to changes in the rate of DAP incorporation. The peaks occurring during the first two generations of elution are larger and with a different shape than the subsequent two peaks. (b) Elution ratio of *N*-[^{3}H]acetylglucosamine to [^{14}C]leucine in *E. coli* NC3 (●).

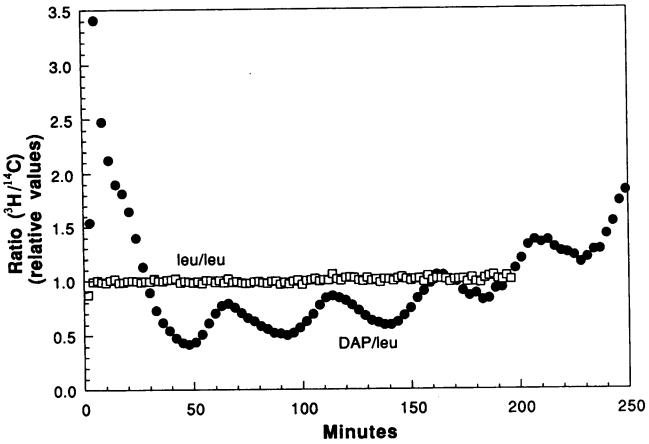

FIG. 4. Test of the variation in the ratio by comparing amino acid incorporation with double label. A membrane elution experiment was performed with [^{3}H]leucine and [^{14}C]leucine. The ratio values were divided by the average ratio value, and the results were plotted (□). The ratio from Fig. 1 for DAP to leucine was normalized the same way and plotted (●). The leucine/leucine ratio experiment was set up so that the actual counts obtained in each fraction were similar to those obtained with the cell surface labels in Fig. 2 and 3.

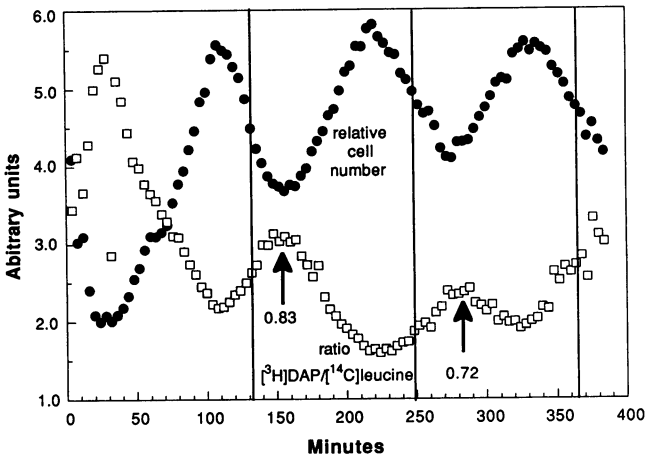

FIG. 5. Membrane elution experiment with *E. coli* NC3 carried out at room temperature (22°C). The cell number elution profile and the [^{3}H]DAP/[^{14}C]leucine ratio are shown. Vertical lines indicate the beginning of each generation of elution; arrows depict the timing (fraction of a division cycle) of the ratio peak.

positioning is correct (see discussion of Fig. 11), but the height is not elevated. We have no explanation for this result at this time, but speculate that there is something about the variation in generation times, combined with some delay in elution of cells in the first generation, that accounts for this phenomenon.

The statistical significance of these variations in the ratio of DAP to leucine incorporation, is provided by a comparison with an experiment with differentially labeled amino acids (Fig. 4). In this figure, it can be seen that the ratio of two amino acids incorporated into the cells (i.e., the ratio of [^{3}H]leucine to [^{14}C]leucine) is a straight line with no distinguishing peaks. In order to make a valid comparison, the ratios in Fig. 4 have been normalized by division with the average ratio from each set of values. The horizontal line for the two amino acids indicates that the peaked pattern when wall label is compared with amino acid label is statistically and experimentally significant.

We propose that the cyclic variations beyond the second generation of elution are due to changes in the rate of side wall peptidoglycan synthesis (in the culture being labeled just prior to being placed on the membrane) during the division cycle. To test this proposal, we have tried to determine whether the timing of the peaks in the ratio that occur during the first two generations of elution (proposed as resulting from pole growth) differs from that of the subsequent ratio peaks (proposed to result solely from side wall synthesis). A theoretical analysis predicts that the peaks in the third and subsequent generations appear as peaks because of a decrease in side wall synthesis during the latter part of the division cycle and may be observed earlier in the later generations of cells eluted from the membrane than peaks in the first two generations of elution (see Discussion). Analysis of some experiments (e.g., Fig. 3a) shows a difference in the peak size and shape between the second and third generations of elution. The third and subsequent ratio peaks appear slightly delayed relative to the second peak, indicating that they are actually earlier in the division cycle eluted from the membrane. In order to establish whether this was the case, we studied the rate of wall synthesis during the division cycle at room temperature (22°C). The lower temperature allows the timing of cell cycle events to be determined more precisely because more samples can be taken during each cycle of elution. The cell number elution profile and dual-label ratio from such an experiment are shown in Fig. 5. There is cyclic variation in the DAP/leucine ratio during the third generation of elution. The beginning of each generation of elution is indicated by the vertical lines (determined from the cell elution plot). Arrows indicate the ratio peaks. In this experiment, the ratio peak occurs at age 0.83 (i.e., 0.83 of a division cycle after the formation of a newborn cell) during the second generation of elution and at age 0.72 during the third generation of elution. Thus, the peak in the ratio during the third generation of elution appears earlier in the division cycle than the peak in the ratio during the second generation of elution. The timings of the peaks in the DAP/leucine ratio for both *E. coli* and *S. typhimurium* for each generation of elution are given in Table 1.

Incorporation of [^{3}H]glycerol into *E. coli* NC3 during the division cycle. In experiments in which bacteria were labeled with [^{3}H]glycerol for 2, 4, and 6 min, over 90% of the label

TABLE 1. Times of the maximal incorporation of cell surface precursors relative to leucine during the division cycles of *E. coli* NC3 and *S. typhimurium* 2616

Bacterium and label	Time of maximal incorporation (fraction of a generation) for[a]:		
	2nd generation	3rd generation	4th generation
E. coli NC3			
[^{3}H]glycerol	0.75 ± 0.05	0.68 ± 0.07	0.68 ± 0.11
[^{3}H]DAP	0.73 ± 0.07	0.68 ± 0.09	ND[b]
[^{3}H]palmitate	0.85 ± 0.04	0.75 ± 0.05	ND
S. typhimurium			
[^{3}H]palmitate	0.74 ± 0.01	0.73 ± 0.04	ND
[^{3}H]DAP	0.73 ± 0.02	0.71 ± 0.04	0.69 ± 0.07

[a] Values are means ± standard deviations.
[b] ND, not determined.

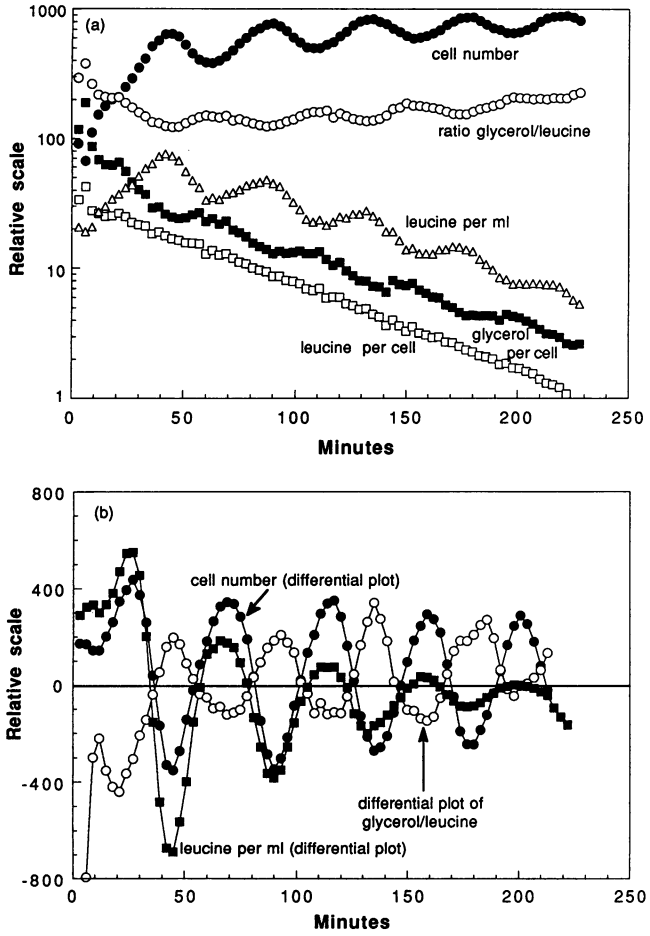

FIG. 6. Glycerol and leucine incorporation during the division cycle of *E. coli* NC3. (a) Plots of cell number, leucine per cell, leucine per milliliter, glycerol per cell, and the ratio of [^{3}H]glycerol to [^{14}C]leucine. Bacteria were labeled with [^{3}H]glycerol and [^{14}C] leucine and filtered onto a membrane, and the membrane elution experiment was set up as described in Materials and Methods. Samples were collected into scintillation vials at 3-min intervals for five generations of elution. The cell number was monitored by Coulter counting. (b) The differential of a running average for the cell number, the leucine per milliliter, and the glycerol/leucine ratio. The differentials were calculated from a running average of three consecutive values. As predicted by the theory and shown in Fig. 1b, the minima for the cell number and the leucine per milliliter occur at similar times. The generations of elution are timed from minimum to minimum and right to left. The timing of the maximum incorporation of glycerol relative to leucine during each generation of elution is determined at the time the ratio is 0 going from maximum to minimum. The average times of peaks in the ratio, utilizing glycerol labeling in *S. typhimurium* 2616, are shown in Table 1.

incorporated into bacteria was extractable with total lipid. This indicated that for short-term labeling experiments, glycerol was a valid label for monitoring phospholipid synthesis. Furthermore, there was no evidence for a significant pool of label, and therefore the rate of uptake of [^{3}H]glycerol was taken as a measure of the rate of phospholipid (membrane) synthesis.

The results from a double-label experiment with [^{3}H]glycerol and [^{14}C]leucine are shown in Fig. 6a. The [^{14}C]leucine per cell decreases exponentially. However, the [^{3}H]glycerol counts per cell, while decreasing, clearly show significant fluctuations during the division cycle. This is also apparent in the ratio of [^{3}H]glycerol to [^{14}C]leucine. The differential of the cell number and leucine per milliliter is shown in Fig. 6b. The minima in the [^{14}C]leucine per milliliter and cell number per milliliter coincide, indicating that the [^{14}C]leucine per milliliter is, in fact as well as in theory (Fig. 1), a measure of generations of elution. The predicted decrease in trough size for the [^{14}C]leucine per cell with each successive generation of elution as shown by Fig. 1b can also be seen in Fig. 6b. The minima of the cell number and leucine per cell differential demarcate the end of a generation of elution. It can be seen that each generation of elution is approximately 45 min, equivalent to the generation time of *E. coli* NC3 before application to the membrane elution apparatus.

The differential of the ratio plot (Fig. 6b) exhibits cell cycle fluctuations. The time of maximal glycerol incorporation (relative to leucine) is when the differential plot of the ratio is 0 (from maxima to minima). Interpreting the graphs from right to left, the peaks in glycerol to leucine incorporation occur towards the end of each division cycle.

In order to measure the timing of peaks in the ratio more precisely, some experiments were carried out at room temperature (22°C). The results of an automated experiment with *E. coli* NC3 at 22°C are shown in Fig. 7. This experiment was performed without monitoring cell number. The [^{3}H]glycerol per milliliter, [^{14}C]leucine per milliliter, and the ratio are shown in Fig. 7a. The differential of the [^{14}C]leucine per milliliter and the ratio are plotted in Fig. 7b. The generations of elution are measured from minimum to minimum (right to left) from the differential of the leucine per milliliter. The times of the peaks in the ratio for the second and third generations of elution are indicated by arrows. Note that the peaks for the ratio differential are indicated where the differential crosses a 0 value, i.e., a 0 slope. The intergeneration time is taken from the minimum of the leucine per milliliter differential, because this is when the end of a generation occurs. Furthermore, note that generational age increases from right to left within each generation, so that the peak age value for the ratio is lower for the third generation (0.64) than for the second generation (0.75). That is, the peak in the third generation appears earlier in the division cycle than the peak in the second generation of elution.

Timings during the division cycle for the peak of glycerol incorporation relative to leucine in *E. coli* NC3 were determined over four generations of elution in four separate experiments. The mean times (as a fraction of the division cycle) are shown in Table 1. Results were difficult to interpret from the first generation of elution because of variations in its elution time.

Incorporation of [^{3}H]palmitate into *S. typhimurium* 2616 and *E. coli* NC3 during the division cycle. The fatty acid [^{3}H]palmitate was used as a radiolabel specific for phospholipids to confirm the results obtained for glycerol. A problem in using this fatty acid with the backwards membrane elution method is that some of the unincorporated palmitate adheres to the nitrocellulose membrane and is not removed upon washing. Some label is therefore available to bacteria on the membrane. This results in a proportion of the eluted label not representing the initial pulse into the bacteria (approximately 10 to 30% in the first generation). Despite this obscuring effect, cyclic variations in the palmitate-/leucine-eluted ratio were clearly visible with both *E. coli* and *S. typhimurium*. The differential plots from double-label experiments with *S. typhimurium* 2616 (Fig. 8) and *E. coli* NC3

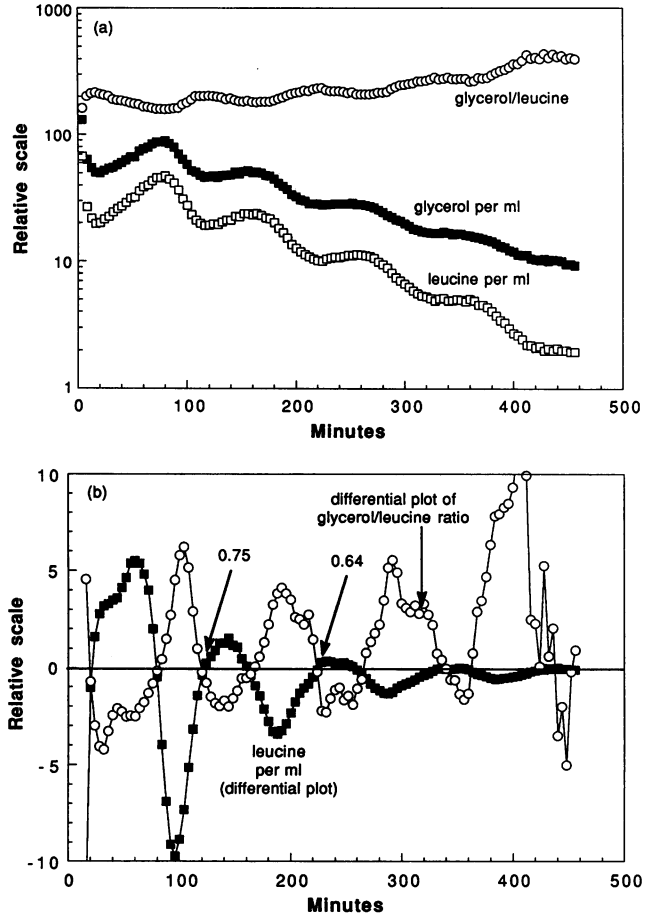

FIG. 7. Incorporation of glycerol and leucine during the division cycle of *E. coli* NC3 at room temperature (22°C). Bacteria were labeled for 6 min and filtered onto a membrane, and the membrane elution experiment was set up as described in Materials and Methods. No cell numbers were monitored during this experiment. (a) Leucine per milliliter, glycerol per milliliter, and the ratio of [^{3}H]glycerol to [^{14}C]leucine. (b) The differential plot of the ratio and leucine per milliliter. The values were calculated from a running average of three consecutive values. The times during the division cycle for the peak in the incorporation of glycerol to leucine for the second and third generations of elution are indicated by the arrows.

(Fig. 9) are shown. The mean times of peaks in the ratio for each generation of elution from four palmitate labeling experiments with *E. coli* NC3 and three palmitate labeling experiments with *S. typhimurium* 2616 are given in Table 1.

Comparison of the incorporation rates of peptidoglycan and phospholipid precursors during the division cycle. The timings of the peaks in the incorporation of DAP to leucine and of glycerol and palmitate to leucine during the division cycle are given in Table 1. The timings are similar, suggesting that membrane and peptidoglycan synthesis have the same pattern during the division cycle.

DISCUSSION

Theoretical considerations related to surface growth during the division cycle. It has been proposed (2, 7) that cells increase their volume in response to the increase in cell mass by elongating the cells at a constant diameter. Prior to

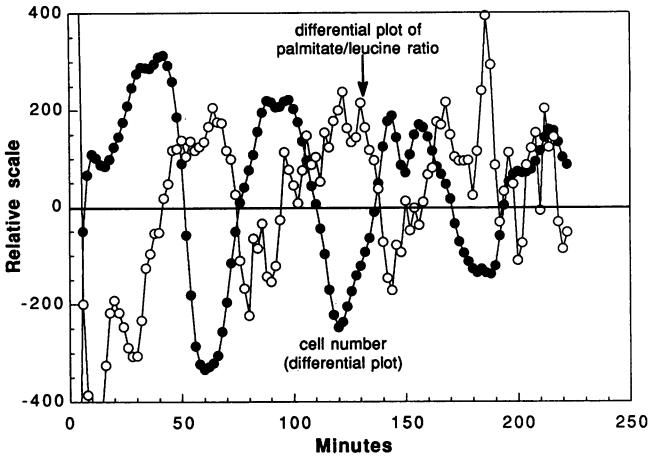

FIG. 8. Palmitate incorporation during the division cycle of *S. typhimurium* 2616. Only the differential of the ratio and the cell number are plotted. The differentials were calculated from a running average of three consecutive values. The average timings of peaks in the ratio are shown in Table 1.

invagination, the ratio of the rate of surface to the rate of mass synthesis is constant. After invagination begins, there is an increase in the ratio of wall increase to cytoplasm increase. This model is illustrated in Fig. 10. The point emphasized here is that during invagination, a decrease in the rate of side wall synthesis is expected. This is because pole growth accommodates some mass growth, thus reducing the need for side wall synthesis.

The predicted pattern for the ratio of wall to protein label for a cell initiating septation halfway through the cell cycle, with pole growing during invagination at a constant rate, is shown in Fig. 11. The peaks in the ratio of wall to protein label during the first two generations are due to the contribution of the pole growth during the latter part of the division cycle. If cells are bound to the membrane at a fixed point, then after two generations the newly synthesizing pole material will have been eluted from the membrane. This can be seen by imagining the cell as bound to the membrane

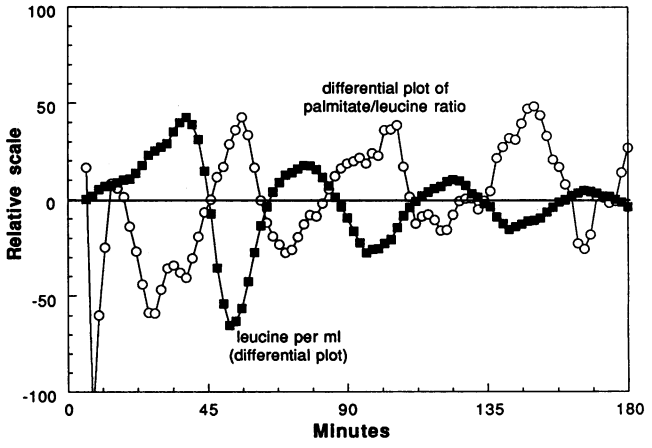

FIG. 9. Palmitate incorporation during the division cycle of *E. coli* NC3. Only the differential of the ratio and leucine per milliliter are plotted. The differentials were calculated from a running average of three consecutive values. The average timings of peaks in the ratio are shown in Table 1.

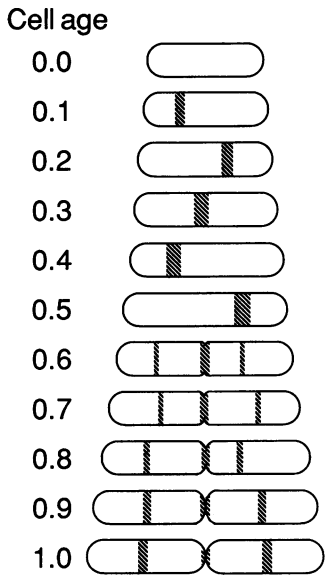

FIG. 10. Proposed model for the rate and topography of peptidoglycan synthesis during the division cycle of a rod-shaped, gram-negative cell. The newborn cell at the top is drawn with a cylinder length of 2.0 and a radius of 0.5; the total length is 3.0 and the dividing cell at the bottom has a length of 6.0. The remaining cells are drawn to scale so that cell volume increases exponentially throughout the division cycle. Before invagination, the cell grows only by side wall cylinder extension. The shaded regions of the cell indicate the amount and location of wall growth (whether in pole or side wall), each 10th of a division cycle. The width of the shaded area is drawn to scale. Cell-surface growth actually occurs throughout the side wall and not in a narrow contiguous zone; the showing of a zone of growth is meant to indicate the quantitive aspects of side wall growth and not to show the precise location of growth. Before invagination, the ratio of the rate-of-surface increase to the rate-of-volume increase is constant. When invagination or pole synthesis begins (age 0.5 in this example), it is assumed that pole synthesis increases linearly such that the surface of the pole increases in equal increments. There is an increase in the ratio of the rate-of-surface increase to the rate-of-volume increase. The predicted pattern of a dual label experiment, expressed as the ratio of wall label to protein label, is shown in Fig. 11. (For detailed discussion see references 2, 4, and 7). Any volume not accommodated by pole growth is accommodated by cylinder growth. At the start of pole growth, there is a reduction in the rate of surface growth in the cylinder. As the pole continues to grow, there is a decrease in the volume accommodated by the pole and there is an increase in the rate of growth in the side wall. This is schematically illustrated by the thinner sector in the expanding side wall immediately after the start of constriction. As the new pole increases, in increments of equal area between the indicated ages, the volume accommodated by the new poles is continuously decreasing. Therefore, the rate of side wall growth in the cylindrical portion increases continuously during the constriction period. At the end of the division cycle, the rate of synthesis in the cylinder is the same as the rate for a newborn cell. There is no sharp change in the rate of cylinder elongation at the instant of division. It should be noted that the cell growth drawn in this figure occurs with a constant diameter. Although diameter varies over many generations, the diameter does not vary in any significant way over a single generation. Thus, while all cells in a population may not have the same diameter, the diameter during the division cycle does not vary (see references 4 and 5 for complete discussion).

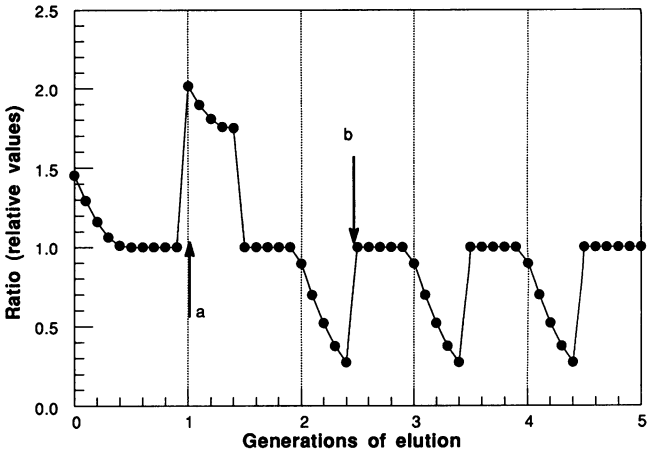

FIG. 11. Expected ratio according to the model of cell growth depicted in Fig. 10. The details of the elution pattern for the first two generations of elution have been described previously (2). The ratios at the third and later generations of elution, where the contributions of new pole synthesis are eliminated, show a repetitive pattern. The loss of labeled pole is assumed to occur because new pole material is made in the center of a dividing cell. After the first two generations of elution, the labeled pole material in the center of the cell will have been lost. Note that the peak labeled a will appear later in the division cycle, occurring between 1 and 2 on the abscissa, compared with the peak labeled b, which occurs between generations 2 and 3 on the abscissa. It is assumed that the variability of the division cycle and differences in timing from those presented in Fig. 10 lead to peaked patterns which only approximate the theoretical predictions.

elution apparatus by an older pole, with a newly labeled pole present in the center of the cell. During the first generation of growth, one of the newly synthesized poles will be lost to the elution medium by division, and during the second generation of elution the other pole will be lost as the bound cell divides in the middle of the cell. Thus, after two generations of elution, only the rate of side wall synthesis will be expected to be measured in the eluate.

Previous experiments detected changes in the rate of peptidoglycan synthesis due to formation of the septum (2, 7). Utilizing a slightly changed methodology with the membrane elution experiments (see Materials and Methods), cyclic variations in the rate of cell surface precursor incorporation relative to leucine incorporation have now been detected beyond the second generation of elution. (It should be noted that previous descriptions of expectations beyond the second generation of elution [e.g., Fig. 6.6 of reference 4] are not correct; the correct predictions are presented here in Fig. 11.)

A consequence of the predicted model is that the peak (or more properly, the plateau) of the ratio graph in the third and subsequent generations of elution may occur earlier in the cell cycle than the peaks in the first and second generations of elution. This theoretical difference is depicted in Fig. 11. The precise predictions of this figure are not to be expected in any set of experiments because the calculations of the graph in Fig. 11 are for cells invaginating at age 0.5 and with pole growth occurring in equal increments of area (Fig. 10). If either the start of invagination or the rate of pole growth differs in the actual cell or if there is a significant variation in the timing of initiation of pole synthesis, one would expect a different ratio pattern. However, a change in the timing of the peaks would still be expected between the 2nd and 3rd

generations of elution. Our results do not demonstrate such a clear difference in peak shape and timing as predicted in Fig. 11, although some differences were observable. Population variation would also effect a smoothing of the data and an obscuring of the changes in timing during the later generations of elution. The clear inverse relationship in our data between the cell number and the ratio implies a close connection between cell age and the ratio change, primarily that the oldest cells of the population exhibit the highest ratio of cell surface precursor to leucine. This connection would be expected to be found at all growth rates. Our objective determinations of the cyclic timings do indicate differences in timing between the second and subsequent generations. The theory of wall synthesis and the predictions to be derived from these calculations are approximate at this time. We point out that there are significant variations in the ratio during the third and subsequent generations of elution and that the timing of the peaks in the ratio is consistent with the proposal that during the latter generations of elution, only side wall synthesis is being observed. Our results are consistent with experiments studying the distribution of grains within individual bacteria radiolabeled with DAP, which demonstrated a reduction in side wall synthesis during invagination (17).

It is possible to measure a small amount of turnover and release of peptidoglycan material from labeled *S. typhimurium* 2616 (6, 8). We have looked for cell cycle-specific release of material from cells, and no evidence for such a phenomenon was detected. Furthermore, the low amount of turnover (on the order of 7% per generation) does not prevent our detection of cell cycle variations in incorporation of peptidoglycan precursors. While such turnover might make the results less obvious, the fact that we see these results despite the potential distractions of turnover suggests that turnover is not a major problem in these experiments.

We conclude from the work presented here (i) that we are measuring the rate of side wall synthesis during the third and subsequent generations of elution, (ii) that there is a decrease in the rate of side wall synthesis during the latter part of the division cycle, and (iii) that the pattern of synthesis observed is consistent with the proposal that mass increase regulates the synthesis of cell surface during the division cycle.

Turning now to the pattern of membrane synthesis, over the past two decades there have been many proposals regarding the pattern of membrane synthesis during the division cycle (9, 10, 15, 16). The previous proposals have not related membrane synthesis to the pattern of peptidoglycan synthesis during the division cycle. Our experiments have shown that membrane synthesis does follow the same cell cycle pattern as peptidoglycan. Pierucci's (15, 16) data on phospholipid synthesis, obtained with the membrane elution method, are also consistent with the rate of phospholipid synthesis being similar to that of peptidoglycan synthesis. However, those data were interpreted in terms of a bilinear pattern similar to that exhibited with thymidine labeling. Our results show a significant increase in the incorporation of membrane (and peptidoglycan) precursors relative to leucine in the latter part of the division cycle. The inverse correlation of the ratio with cell number supports the proposal that there is a decrease in the rate of cell surface synthesis at division. This correlation argues against a doubling in the rate of synthesis in the middle of the division cycle. Such an event during the division cycle gives a well-defined plateau in the eluted counts per cell and a sharper inverted sawtooth pattern in the ratio (as with thymidine; unpublished data). We propose that the stress-bearing peptidoglycan layer enlarges in response to mass accumulation. In turn, cell membrane grows passively in response to the increase in peptidoglycan surface and coats the peptidoglycan with minimal stretching and buckling.

For completeness, we would note that an alternative argument could be made that membrane responds to the turgor pressure and that peptidoglycan biosynthesis follows membrane expansion. The main argument against this view is that dissolution of the peptidoglycan by enzymes leads to cell lysis because the membrane is not structurally strong enough to hold the cell together. Thus, to have membrane be the rate-limiting component on cell expansion is difficult to imagine at this time.

Our data do not allow us to clearly distinguish between different proposals for the rate of membrane synthesis during the division cycle. The rate is not exponential and is not consistent with the pattern expected for a bilinear mode of synthesis. Here, we stress that there is a good correlation of the pattern of membrane synthesis with the pattern of peptidoglycan synthesis.

There is good agreement between our experimental observations and the theoretical pattern of surface synthesis based on mass-driven expansion. Until there are either experiments capable of clearly differentiating between the different models or a better theory that accommodates the available data, we propose that the cell surface—including both membrane and peptidoglycan—increases to maintain a constant cell density in response to an exponential mass increase.

ACKNOWLEDGMENTS

The preparation of this article and the experiments within were supported by National Institutes of Health grant R01 GM44022-01A1.

REFERENCES

1. **Bligh, E. G., and W. J. Dyer.** 1959. A rapid method of total lipid extraction and purification. Can. J. Biochem. Physiol. **37**:911–917.
2. **Cooper, S.** 1988. Rate and topography of cell wall synthesis during the division cycle of *Salmonella typhimurium*. J. Bacteriol. **170**:422–430.
3. **Cooper, S.** 1988. Leucine uptake and protein synthesis are exponential during the division cycle of *Escherichia coli* B/r. J. Bacteriol. **170**:436–438.
4. **Cooper, S.** 1991. Bacterial growth and division: biochemistry and regulation of the division cycle of prokaryotes and eukaryotes. Academic Press, Inc., San Diego, Calif.
5. **Cooper, S.** 1991. Synthesis of the cell surface during the division cycle of rod-shaped, gram-negative bacteria. Microbiol. Rev. **55**:1649–1674.
6. **Cooper, S., D. Gally, Y. Suneoka, M. Penwell, K. Caldwell, and K. Bray.** 1992. Peptidoglycan synthesis in *Salmonella typhimurium*, p. 161–168. *In* Bacterial growth and lysis, metabolism and structure of the bacterial sacculus. Plenum Publishing Co., New York.
7. **Cooper, S., and M.-L. Hsieh.** 1988. The rate and topography of cell wall synthesis during the division cycle of *Escherichia coli* using *N*-acetylglucosamine as a peptidoglycan label. J. Gen. Microbiol. **134**:1717–1721.

7a. **Cronan, J. E., Jr., and C. O. Rock.** 1987. Biosynthesis of membrane lipids, p. 474–497. *In* F. C. Neidhardt, J. L. Ingraham, K. B. Low, B. Magasanik, M. Schaechter, and H. E. Umbarger (ed.), *Escherichia coli* and *Salmonella typhimurium*. American Society for Microbiology, Washington, D.C.

8. **Herman, D., D. Gally, K. Bray, and S. Cooper.** Unpublished results.
9. **Joseleau-Petit, D., F. Képès, and A. Képès.** 1984. Cyclic changes of the rate of phospholipid synthesis during synchronous growth

of *Escherichia coli*. Eur. J. Biochem. **139:**605–611.
10. **Joseleau-Petit, D., F. Képès, L. Peutat, R. D'Ari, and A. Képès.** 1987. DNA replication initiation, doubling of rate of phospholipid synthesis, and cell division in *Escherichia coli*. J. Bacteriol. **169:**3701–3706.
11. **Joseleau-Petit, D., F. Képès, L. Peutat, R. D'Ari, and L. I. Rothfield.** 1990. Biosynthesis of membrane adhesion zone fraction throughout the cell cycle of *Escherichia coli*. J. Bacteriol. **172:**6573–6575.
12. **Koch, A. L.** 1983. The surface stress theory of microbial morphogenesis. Adv. Microbiol. Physiol. **24:**301–366.
13. **Koch, A. L., and S. Woeste.** 1992. Elasticity of the sacculus of *Escherichia coli*. J. Bacteriol. **174:**4811–4819.
14. **Kubitschek, H. E.** 1987. Buoyant density variation during the cell cycle in microorganisms. Crit. Rev. Microbiol. **14:**73–97.
15. **Pierucci, O.** 1979. Phospholipid synthesis during the cell division cycle of *Escherichia coli*. J. Bacteriol. **138:**453–460.
16. **Pierucci, O., M. Melzer, C. Querini, M. Rickert, and C. Krajewski.** 1981. Comparison among patterns of macromolecular synthesis in *Escherichia coli* B/r at growth rates of less and more than one doubling per hour at 37°C. J. Bacteriol. **148:**684–696.
17. **Woldringh, C. L., P. Huls, E. Pas, G. J. Brakenhoff, and N. Nanninga.** 1987. Topography of peptidoglycan synthesis during elongation and polar cap formation in a cell division mutant of *Escherichia coli* MC4100. J. Gen. Microbiol. **133:**575–586.
18. **Zaritsky, A., and C. Helmstetter.** Unpublished results.